DEVELOPMENT AND VALIDATION OF A REDUCED ONE-DIMENSIONAL THERMO-MECHANICAL SOIL STABILITY MODEL

For Predictive use with the Alaska RWIS

FINAL PROJECT REPORT

by

Rorik A Peterson, PI
Assoc. Professor of Mechanical Engineering
University of Alaska Fairbanks

Michael Stoddard
Graduate Research Assistant
University of Alaska Fairbanks

for

Center for Safety Equity in Transportation (CSET)
USDOT Tier 1 University Transportation Center
University of Alaska Fairbanks
ELIF Suite 240, 1764 Tanana Drive
Fairbanks, AK 99775-5910

In cooperation with U.S. Department of Transportation,
Research and Innovative Technology Administration (RITA)

DISCLAIMER

The contents of this report reflect the views of the authors, who are responsible for the facts and the accuracy of the information presented herein. This document is disseminated under the sponsorship of the U.S. Department of Transportation's University Transportation Centers Program, in the interest of information exchange. The Center for Safety Equity in Transportation, the U.S. Government and matching sponsor assume no liability for the contents or use thereof.

TECHNICAL REPORT DOCUMENTATION PAGE

1. Report No.	2. Government Accession No.	3. Recipient's Catalog No.

4. Title and Subtitle	5. Report Date
Development and validation of a reduced one-dimensional thermos-mechanical soil stability model for predictive use with the Alaska RWIS	7/10/2024
	6. Performing Organization Code

7. Author(s) and Affiliations	8. Performing Organization Report No.
Rorik Peterson Univ. of Alaska Fairbanks Michael Stoddard Univ. of Alaska Fairbanks	INE/CSET 24.13

9. Performing Organization Name and Address	10. Work Unit No. (TRAIS)
Center for Safety Equity in Transportation ELIF Building Room 240, 1760 Tanana Drive Fairbanks, AK 99775-5910	11. Contract or Grant No.

12. Sponsoring Organization Name and Address	13. Type of Report and Period Covered
United States Department of Transportation Research and Innovative Technology Administration 1200 New Jersey Avenue, SE Washington, DC 20590	14. Sponsoring Agency Code

15. Supplementary Notes

Report uploaded to:

16. Abstract

A numerical tool was developed that helps forecast when thaw occurs at depths in a road embankment during spring thaw in regions that experience seasonal freeze and thaw. The tool is a Excel spreadsheet that uses a single adjustable parameter, and is driven by time series air temperature data. The model agrees well with archived data of subsurface temperatures at five different highway locations in Alaska.

17. Key Words	18. Distribution Statement		
Frigid regions, thaw, predictive models, road embankment			
19. Security Classification (of this report)	**20. Security Classification (of this page)**	**21. No. of Pages**	**22. Price**
Unclassified.	Unclassified.	21	N/A

Form DOT F 1700.7 (8-72) **Reproduction of completed page authorized.**

SI* (MODERN METRIC) CONVERSION FACTORS

APPROXIMATE CONVERSIONS TO SI UNITS				
Symbol	**When You Know**	**Multiply By**	**To Find**	**Symbol**
		LENGTH		
in	inches	25.4	millimeters	mm
ft	feet	0.305	meters	m
yd	yards	0.914	meters	m
mi	miles	1.61	kilometers	km
		AREA		
in^2	square inches	645.2	square millimeters	mm^2
ft^2	square feet	0.093	square meters	m^2
yd^2	square yard	0.836	square meters	m^2
ac	acres	0.405	hectares	ha
mi^2	square miles	2.59	square kilometers	km^2
		VOLUME		
fl oz	fluid ounces	29.57	milliliters	mL
gal	gallons	3.785	liters	L
ft^3	cubic feet	0.028	cubic meters	m^3
yd^3	cubic yards	0.765	cubic meters	m^3
	NOTE: volumes greater than 1000 L shall be shown in m^3			
		MASS		
oz	ounces	28.35	grams	g
lb	pounds	0.454	kilograms	kg
T	short tons (2000 lb)	0.907	megagrams (or "metric ton")	Mg (or "t")
		TEMPERATURE (exact degrees)		
°F	Fahrenheit	5 (F-32)/9 or (F-32)/1.8	Celsius	°C
		ILLUMINATION		
fc	foot-candles	10.76	lux	lx
fl	foot-Lamberts	3.426	$candela/m^2$	cd/m^2
		FORCE and PRESSURE or STRESS		
lbf	poundforce	4.45	newtons	N
lbf/in^2	poundforce per square inch	6.89	kilopascals	kPa

APPROXIMATE CONVERSIONS FROM SI UNITS				
Symbol	**When You Know**	**Multiply By**	**To Find**	**Symbol**
		LENGTH		
mm	millimeters	0.039	inches	in
m	meters	3.28	feet	ft
m	meters	1.09	yards	yd
km	kilometers	0.621	miles	mi
		AREA		
mm^2	square millimeters	0.0016	square inches	in^2
m^2	square meters	10.764	square feet	ft^2
m^2	square meters	1.195	square yards	yd^2
ha	hectares	2.47	acres	ac
km^2	square kilometers	0.386	square miles	mi^2
		VOLUME		
mL	milliliters	0.034	fluid ounces	fl oz
L	liters	0.264	gallons	gal
m^3	cubic meters	35.314	cubic feet	ft^3
m^3	cubic meters	1.307	cubic yards	yd^3
		MASS		
g	grams	0.035	ounces	oz
kg	kilograms	2.202	pounds	lb
Mg (or "t")	megagrams (or "metric ton")	1.103	short tons (2000 lb)	T
		TEMPERATURE (exact degrees)		
°C	Celsius	1.8C+32	Fahrenheit	°F
		ILLUMINATION		
lx	lux	0.0929	foot-candles	fc
cd/m^2	$candela/m^2$	0.2919	foot-Lamberts	fl
		FORCE and PRESSURE or STRESS		
N	newtons	0.225	poundforce	lbf
kPa	kilopascals	0.145	poundforce per square inch	lbf/in^2

*SI is the symbol for the International System of Units. Appropriate rounding should be made to comply with Section 4 of ASTM E380.
(Revised March 2003)

TABLE OF CONTENTS

LIST OF FIGURES

LIST OF TABLES

EXECUTIVE SUMMARY

Seasonal vehicular weight road restrictions are often used in Northern climates to mitigate the damage that can occur in spring during thaw. Frost heave and related freeze/thaw processes in wet soil decrease the compressive strength of highways. The location of the frozen/unfrozen interface is a primary determinant for the physical stability of the overlying material. The Alaska Dept. of Transportation and Public Facilities (ADOT&PF) generally apply weight restrictions during spring thaw until the thaw depth reaches five feet. ADOT&PF maintains a system of Road Weather Information Stations (RWIS) that record air and subsurface temperatures in order to know approximately when this occurs. There are some limitations to relying on RWIS sites for determination of seasonal commercial vehicle weight restrictions, such as cost and the associated limited number of sites over a large geographic area. A numerical model was developed as a one-dimensional finite difference thermal energy balance that accounts for both sensible and latent heat effects in a semi-saturated soil. The primary goal was to accurately forecast the time when specific vertical locations thaw; specifically, 1 foot and 5 feet below surface in this case. The tool is in the form of an Excel spreadsheet and requires only a single adjustable parameter that represents a modified thermal diffusivity that accounts for latent heat effects. The model is driven using air temperature data, and predicts the temperature at depth. The time resolution of the model is the same as the input temperature data. The model was calibrated and evaluated using archived RWIS data at five locations in Alaska with 1 hour resolution. The same value for apparent thermal diffusivity was used at all sites. The average error at 1 foot depth was 4.78 days, and 8.5 days at 5 feet depth. The spreadsheet tool does not include any macros or external scripts, so can be used in most other major spreadsheet programs such as Libreoffice Calc.

CHAPTER 1. INTRODUCTION

Seasonal vehicular weight road restrictions are often used in Northern climates to mitigate the damage that can occur in spring during thaw. Frost heave and related freeze/thaw processes in wet soil decrease the compressive strength of highways. Frozen ground contains ice in different forms ranging micron-scale soil particle coatings to millimeter-scale ice inclusions. When thawing, the associated volume-contraction of water leads to a decrease in mechanical strength of the highway. The overburden pressure of vehicle traffic causes the soil skeleton to adapt. Concurrently, the excess pore pressure eventually decreases as liquid drains; and the rate is a function of the solid material physical characteristics and the thermal regime.

The location of the frozen/unfrozen interface is a primary determinant for the physical stability of the overlying material. Its relative impermeability severely impedes relaxation of the excess pore water pressure. Therefore, depth-of-thaw location is conventionally used as an indicator for a highway's seasonally changing mechanical strength. The thaw depth can be measured automatically in near-real time using temperature depth probes (TDP), which are most often a string of thermistors embedded in a rigid rod at strategically determined depth locations along the probe rod.

The Alaska Dept. of Transportation and Public Facilities (ADOT&PF) maintains a system of Road Weather Information Stations (RWIS) along the primary highway system in Alaska. Each station includes an Environmental Sensor Station (ESS) that measures and records atmospheric, surface/sub-surface, and water/snow conditions at the site. A TDP is used to measure the depth of thaw. The TDPs in the Alaska RWIS system have thermistors located at 3-inch intervals for the first foot below surface, and then 6-inch intervals for an additional five feet of depth. Data collected by the ESS are collected by a remote processing unit at the RWIS, and then transmitted every 6 hours via telephone (where available) or an alternative wireless communication system. A subset of the collected ESS data is then made available in graphical and tabular form on the web through the main AKDOT&PF portal.

There are some limitations and weaknesses in the current use of TDP measurements at RWIS sites for determination of highway material strength and therefore seasonal commercial vehicle weight restrictions. One limitation is the finite and few number of RWIS locations throughout the geographically large Alaska highway system. Clearly the financial cost of installing and maintaining each station limits the number and density of sites. Another limitation is the finite number and spacing between thermistor sensors, which results in a somewhat low-resolution measurement of the actual frost depth. Finally, equipment failure of TDPs results is not uncommon, yet difficult to repair timely if at all. There are also weaknesses in using only depth of thaw as the determining factor for weight restrictions. Various subgrade aggregate materials and natural soils both drain at different rates, as well as have differing cohesive strengths as functions of water content and pore pressure.

1.1. Road Materials

The soil used under highways is typically carefully selected and engineered to provide a stable foundation for the road structure. This subgrade is typically native soil upon which the road is built. It's often compacted and sometimes treated to improve its properties. Ideal subgrade soils are well-draining and have good bearing capacity.

Above the subgrade is the sub-base. This is typically gravel, crushed stone, and/or sand. The sub-base helps with drainage and provides a stable platform for the base course. In areas where the native soil is unsuitable, engineered fill may be used. This is specially selected or treated soil that meets specific engineering requirements.

Key characteristics of soils used under highways include good drainage properties, high bearing capacity, low frost susceptibility, minimal shrink-swell potential, and compactability to achieve desired density. The exact type and composition of soil used can vary based on local availability, climate conditions, traffic load expectations, and regional engineering practices.

1.2. RWIS System

The RWIS system, or Road Weather Information System, is a network of environmental sensor stations used to collect and disseminate road weather data. It's a crucial tool for highway maintenance and safety, especially in regions with challenging weather conditions. RWIS stations typically collect air temperature, humidity, wind speed and direction, precipitation type and intensity, pavement temperature, subsurface temperatures, and sometime pavement condition (e.g. wet, dry, icy). RWIS systems play a crucial role in managing roads in areas prone to freezing, helping to prevent accidents and optimize maintenance efforts. They provide real-time and forecast information that is valuable for both immediate operational decisions and long-term planning. RWIS provides crucial data that helps road maintenance teams make informed decisions about how to manage these conditions.

1.3. Project Goals

The numerical model developed in this project is a one-dimensional finite difference thermal energy balance that accounts for both sensible and latent heat effects in a semi-saturated soil. The primary goal was to accurately forecast the time when specific vertical locations thaw; specifically, 1 foot and 5 feet below surface in this case.

The number of initial input parameters into the model were kept as small as possible. Initially the set would include the physical properties of the underlying soil materials (thermal conductivity, heat capacity, and density). Effective freezing and thawing indices (n-factors) will be determined using archived RWIS data of temperature profiles over time. Effective surface temperatures can then be matched to air temperatures for a top-surface boundary condition into the one-dimensional model.

Initial validation of the model involved comparison of the model forecasts with several years of archived Alaska RWIS data from TDP measurement sites. We worked with Alaska DOT&PF for acquisition of the data, and to gain an understanding of the conditions at each of the RWIS locations. The model validation metrics were deviation between forecast and recorded temperatures with focus on temperatures near freeze/thaw. Model design iteration included reducing the model input requirements such that it can be modified and implemented efficiently for use in a wide range of locations. The ulterior motive of this step is to be applicable to locations far from any current RWIS installations. After the development, validation, and iteration steps, the forecast system wasdesigned for facile integration with the current Alaska RWIS data system.

CHAPTER 2. LITERATURE REVIEW

One-dimensional finite difference models (FDMs) have become a cornerstone for simulating the freezing process in soils. FDMs have been widely employed to simulate one-dimensional freezing processes in soils due to their relative simplicity and computational efficiency. This review explores the strengths and limitations of FDMs in this context, highlighting key considerations for model development and application. This review examines key developments and applications of these models in geotechnical engineering and permafrost studies.

Heat transfer in soil freezing is governed by the heat equation, incorporating latent heat release during water-to-ice phase change. FDMs discretize the spatial domain (usually depth) and time domain, approximating the temperature distribution within the soil profile. Early models often assumed a constant soil composition and a single freezing point for all water (Jumikis, 1977). However, advancements incorporated the dependence of unfrozen water content and thermal properties on temperature (Kozlowski, 2001; Riseborough & Smith, 1985). This improved the accuracy of frost depth prediction, a crucial parameter in geotechnical engineering.

The complexity of FDMs for soil freezing can vary. Simpler models may focus solely on heat transfer, while more sophisticated approaches couple heat and mass transfer to account for water movement during freezing (Comes-Pintaux & Nguyen-Lamba, 1986). The selection depends on the specific problem being addressed and the desired level of detail.

Several factors influence the accuracy and applicability of FDMs. Mesh resolution (spatial and temporal discretization) is critical, as finer meshes lead to more accurate results but require greater computational resources. Furthermore, reliable soil property data, including thermal conductivity, volumetric heat capacity, and the relationship between unfrozen water content and temperature, are essential for accurate simulations (Goodrich, 1978) (Harlan, 1973).

Validation of FDM simulations is crucial. Comparisons with analytical solutions (for simple cases) or field measurements provide confidence in the model's performance. FDMs have been successfully applied to various problems, including predicting frost depth in foundations, evaluating the effectiveness of ground freezing techniques, and understanding the impact of climate change on permafrost. Early work by Harlan (1973) established a foundation for modeling coupled heat and mass transfer in freezing soils using finite difference methods. His model incorporated both conductive and convective heat transfer, as well as moisture migration driven by temperature gradients. Nixon (1975) considered the role of convective heat transport in the thawing of frozen soil. He concluded that for a wide range of conditions, the effect is minor and does not play a significant role in determining the rate of thaw.

Subsequent research focused on improving the representation of soil properties and phase change dynamics. Jame & Norum (1980) developed a model that accounted for the variation of unfrozen water content with temperature, a crucial factor in accurately simulating frost heave and thaw settlement. Konrad & Morgenstern (1984) introduced the segregation potential concept to model frost heave, which was later incorporated into finite difference schemes by various researchers. This approach allowed for more accurate prediction of frost heave in frost-susceptible soils.

Recent advancements have focused on incorporating more complex phenomena and improving numerical stability. Hansson, et al. (2004) developed a model that accounts for salt transport and its

effects on freezing point depression, which is particularly relevant for coastal and saline soils. Dall-Amico, et al. (2011) presented a robust numerical scheme for solving the coupled heat and water flow equations in freezing soils, addressing issues of convergence and stability in previous models. Current research trends include the integration of finite difference models with other numerical techniques, such as finite element methods, to handle more complex geometries and multidimensional problems.

2.1. Latent Heat of Fusion

The latent heat of fusion is a critical component in finite difference models of soil freezing, as it represents the energy required for phase change between water and ice. The apparent heat capacity method is one of the most common approaches. The latent heat is incorporated into an "apparent" or "effective" heat capacity of the soil-water-ice system. The heat capacity is treated as a function of temperature, with a large spike around the freezing point to represent the latent heat effect. This method, used by researchers like Hansson et al. (2004), allows for a smooth transition between frozen and unfrozen states.

Some models, like those based on Harlan's (1973) work, treat the latent heat as a source or sink term in the heat transfer equation. As freezing occurs, the latent heat is released (acting as a heat source), and during thawing, it's absorbed (acting as a heat sink).

This enthalpy formulation, employed by Dall'Amico et al. (2011), uses enthalpy as the primary variable instead of temperature. The enthalpy includes both sensible and latent heat, allowing for a more natural incorporation of phase change effects.

In models that explicitly track the freeze-thaw interface, like Nixon's (1975), the latent heat is accounted for as a boundary condition at the moving frost front. This approach is particularly useful for sharp freeze-thaw interfaces. Many models incorporate the relationship between unfrozen water content and temperature. This indirectly accounts for latent heat effects, as the gradual release of latent heat is reflected in the changing unfrozen water content over a range of sub-zero temperatures.

The choice of method often depends on the specific problem, soil characteristics, and desired balance between computational efficiency and accuracy. More recent models tend to use combinations of these approaches to better represent the complex thermodynamics of freezing soils.

CHAPTER 3. DATA AND METHODS

Determining the physical properties of soil is crucial for accurate finite difference modeling of freezing processes. Models typically handle soil properties in a variety of ways. Many models rely on experimentally determined soil properties as input parameters. These may include thermal conductivity, heat capacity, hydraulic conductivity, porosity, bulk density and particle size distribution. Researchers often conduct laboratory tests on soil samples to obtain these properties before running simulations.

Some properties, particularly thermal properties, are often represented as functions of temperature and phase composition. For example, thermal conductivity is often modeled using weighted averages of soil components (solid particles, water, ice, air) based on volume fractions, which change with temperature. Heat capacity can be similarly calculated using mixture models, accounting for changing proportions of water and ice.

The critical relationship between temperature and unfrozen water content is typically determined experimentally for specific soil types. It's often represented by empirical functions (i.e. unfrozen water curve) or lookup tables in the models.

Some models use parameterization schemes to estimate properties based on soil classification (e.g., sand, silt, clay percentages) and other basic soil data. Often, initial estimates of soil properties are refined through model calibration against field or laboratory data, improving the accuracy of simulations.

It's worth noting that the accuracy of many models heavily depends on the quality and appropriateness of the soil property inputs. Sensitivity analyses are often performed to understand how uncertainties in soil properties affect model outcomes. It was beyond the scope of this project to obtain physical samples and measure physical properties at the sites being studied. Furthermore, it aligns with the overall project goal to keep input parameters to a minimum. Therefore, the initial approach, which was also the final product, required only the thermal diffusivity of the material

$$\alpha = \frac{k}{\rho\, c_p}$$

Furthermore, this value remained the same at all sites investigated. This was not unexpected since the material physical properties down to 5 feet are very similar at all locations.

3.1. Numerical Methods

This model solves the unsteady, one-dimensional heat conduction equation

$$\frac{\partial T}{\partial t} = \alpha \frac{\partial^2 T}{dz^2}$$

by the finite difference method. The latent heat of fusion accounted for using the apparent heat capacity method since tracking the location of the freezing interface would be very difficult with the course resolution and fixed grid of this model.

The entire model is contained in a single Microsoft Excel spreadsheet and contains no macros or other external functions and methods. The only required temperature input into the model is the RWIS

measured air temperature as a function of time. Using that value, the temperature at the following depths (in feet) are calculated: 0.25, 0.5. 0.75, 1.0,1.5, 2.0, 2.5, 3.0, 3.5, 4.0, 4.5, 5.0, 5.5.

The upper most depths were able to be adequately determined without needing to account for latent heat effects. Down to the 1.0 feet depth, the temperature can be determined by an analytic solution of one-dimensional, time-dependent conduction equation with constant physical properties.

$$\frac{T(z,t) - T_i}{T_s - T_i} = erfc\left(\frac{z}{2\sqrt{\alpha\, t}}\right)$$

where T_s is the temperate at the cell directly above it, and T_i is the temperature of the same cell in the time step before current. Below this depth, the thermal diffusivity is determined by a conditional test using the temperature relative to the freezing point.

3.2. RWIS Data

Archived surface and sub-surface temperature data were acquired through the Alaska Department of Transportation and Public Facilities Road Weather Information System website at https://roadweather.alaska.gov/gis.. For all five of the sites used in this study, six years of historical temperature data was acquired. This data included air temperature and ground temperature at all the depths given above. The input to the model is the air temperature, and the remaining ground temperatures were used for development, adjustment and tuning of the model.

3.3. Thermal Model Spreadsheet Tool

This section is a brief visual overview of what the thermal model spreadsheet tool looks like to the end user. Note that the actual sheet may have up to 10,000 columns depending on the time resolution and duration of the data. Time increments of 1.0 hours were used in the development of this tool. Different time increments can be entered for the air temperature, however, and it can be either regularly or irregularly spaced.

Only the left-most part of a single tab of the spreadsheet is usually shown in most of the figures below. Figure 1 shows an overview of what the Excel spreadsheet looks to the user. One visual effect added to the cell data background was color coding from blue to red (cold to warm). For model validation, the actual RWIS data at all depths is included in the data block below the model forecasts. The top block of cell is the model forecast, and the block below that is the actual measure temperature. The top scatter plot is the temperature at 1.0 feet showing both the model and actual measurement, and the plot below that is the same for 5.0 feet depth.

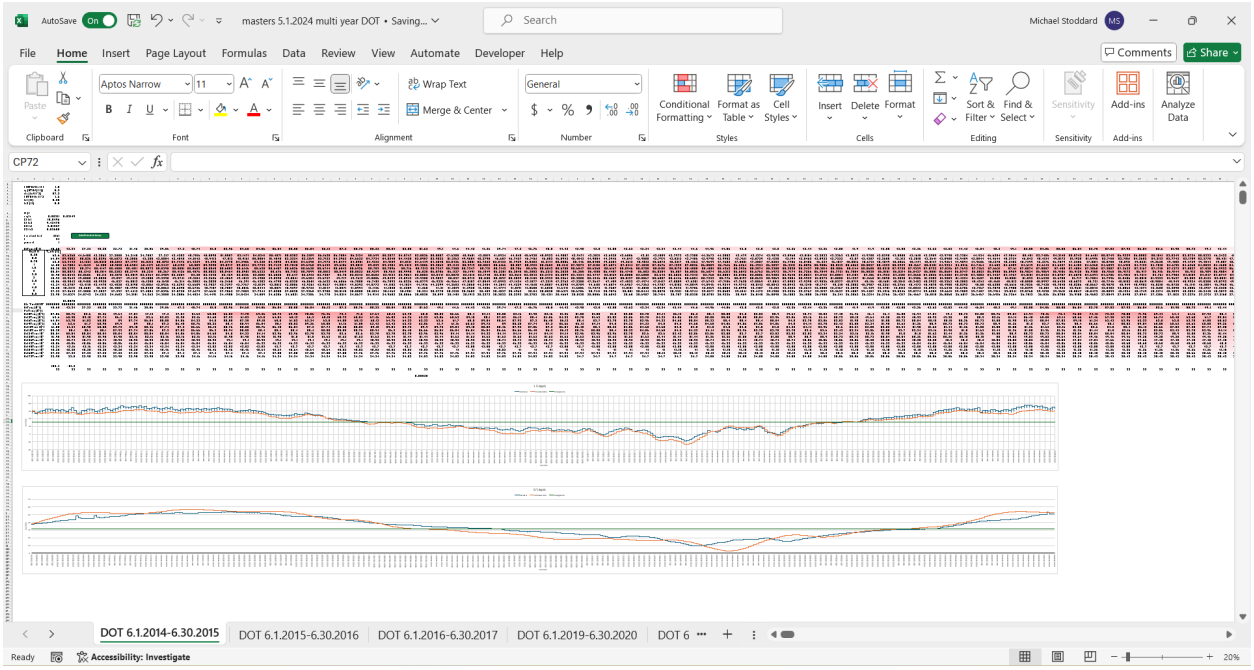

Figure 1 Overview of the model interface

Figure 2 shown below is a closer view of the model data block using background color coding to aid in quick visualization of where the freezing interface is located. Red colors are above freezing, and blue colors are below freezing. Each column represents a time difference of 1.0 hours, and the rows are at the depths given earlier (most are 0.5-foot increments). In this figure, a general idea of the descending freezing front can be seen in the white band.

Day		265	266	267	268	269	270	271	272	273	274	275	276	277	278	279	280	281	282	283	284	285	286	287	288	289	290	291
T_Surface (F)		36.6668	36.061168	35.45227	34.84027	34.22536	33.60773	32.98755	32.365	31.74028	31.11356	30.48504	29.85489	29.2233	28.59047	27.95657	27.3218	26.68634	26.05039	25.41412	24.77773	24.14141	23.50533	22.86971	22.23471	21.60053	20.96736	20.33537
Depth ft	T_initial (F)																											
0.25	39.8	36.4272921	35.54774	34.90955	34.29236	33.67477	33.05484	32.43256	31.80807	31.18157	30.55324	29.92327	29.29185	28.65915	28.02537	27.3907	26.75532	26.11942	25.48319	24.84681	24.21048	23.57439	22.93871	22.30365	21.66938	21.0361	20.40399	
0.5	41.1	37.0406161	35.76101	35.01924	34.37968	33.75778	33.13727	32.51512	31.89089	31.26466	30.63658	30.00683	29.37561	28.74308	28.10945	27.47491	26.83962	26.2038	25.56762	24.93127	24.29494	23.65882	23.02309	22.38796	21.75359	21.12018	20.48793	
0.75	41.9	37.7425306	36.11177	35.20642	34.50787	33.86694	33.24078	32.61719	31.9928	31.36675	30.73894	30.10946	29.47848	28.84618	28.21275	27.57836	26.94321	26.30749	25.67138	25.03507	24.39875	23.7626	23.12683	22.49161	21.85713	21.22358	20.59114	
1	43.1	38.7175831	36.68458	35.5363	34.7201	34.02753	33.38003	32.74807	32.12061	31.49362	30.86567	30.23635	29.60562	28.97358	28.34039	27.70621	27.07124	26.43565	25.79964	25.16339	24.5271	23.89094	23.25512	22.6198	21.9852	21.35148	20.71885	
1.5	44.6	40.6689957	38.26738	36.68965	35.55517	34.65863	33.88932	33.18757	32.52129	31.87321	31.23414	30.59918	29.96577	29.33263	28.69913	28.06505	27.43034	26.79505	26.15932	25.52328	24.88711	24.25098	23.61509	22.97961	22.34472	21.71063	21.0775	
2	45.9	42.7027983	40.34668	38.55733	37.14963	35.99866	35.02018	34.15736	33.37191	32.63804	31.93841	31.26135	30.59907	29.94636	29.29977	28.65701	28.01663	27.37768	26.73961	26.10208	25.46495	24.82816	24.19174	23.55579	22.92041	22.28575	21.65196	
2.5	46.9	44.5312097	42.54704	40.86275	39.41217	38.14363	37.01679	36.00015	35.06917	34.20469	33.39177	32.6188	31.87672	31.15852	30.45875	29.77318	29.09856	28.43239	27.77276	27.11821	26.46764	25.82024	25.17541	24.53273	23.89191	23.25275	22.61517	
3	47.9	46.2447601	44.73581	43.35227	42.0762	40.89218	39.787	38.7493	37.76934	36.83876	35.95042	35.09818	34.27678	33.48176	32.70926	31.95601	31.21924	30.49656	29.78596	29.08573	28.39445	27.71088	27.03401	26.363	25.69714	25.03585	24.37865	
3.5	48.6	47.5346051	46.508	45.51662	44.55723	43.62687	42.72288	41.84279	40.98441	40.1457	39.32486	38.52022	37.73028	36.95369	36.18923	35.43578	34.69237	33.95808	33.23212	32.51377	31.80239	31.09741	30.39832	29.70468	29.01609	28.3322	27.65273	
4	49.1	48.4611743	47.82381	47.1877	46.55262	45.9184	45.28486	44.65186	44.01927	43.38697	42.75485	42.12283	41.49083	40.85879	40.22666	39.59439	38.96198	38.32938	37.69661	37.06366	36.43055	35.79729	35.16391	34.53046	33.89697	33.26349	32.63009	
4.5	49.7	49.334765	48.963	48.58481	48.20028	47.8095	47.41259	47.00963	46.60073	46.186	45.76554	45.33947	44.90789	44.47093	44.02869	43.58129	43.12886	42.67152	42.20938	41.74258	41.27123	40.79548	40.31545	39.83126	39.34306	38.85097	38.35514	
5	50.4	50.2012263	49.99677	49.78666	49.57094	49.34965	49.12283	48.89052	48.65277	48.40963	48.16115	47.90738	47.64837	47.38417	47.11486	46.84047	46.56109	46.27675	45.98754	45.69352	45.39475	45.09131	44.78326	44.47067	44.15363	43.83221	43.50648	
5.5	50.7	50.6005761	50.49769	50.39135	50.28155	50.16831	50.05162	49.9315	49.80795	49.68098	49.5506	49.41683	49.27968	49.13917	48.9953	48.8481	48.69758	48.54376	48.38667	48.22632	48.06274	47.89596	47.72598	47.55285	47.37659	47.19722	47.01478	

Figure 2 Closer view of the data blocks with background color coding

Figure 3 simply illustrates a user interfacing with the model. User adjustable parameters are in the upper left. There are a few cells below those that were used for development and tuning of the model and can be hidden or even completely removed by the user if desired. Time data are entered in a single row of the model in any resolution available to or desired by the user.

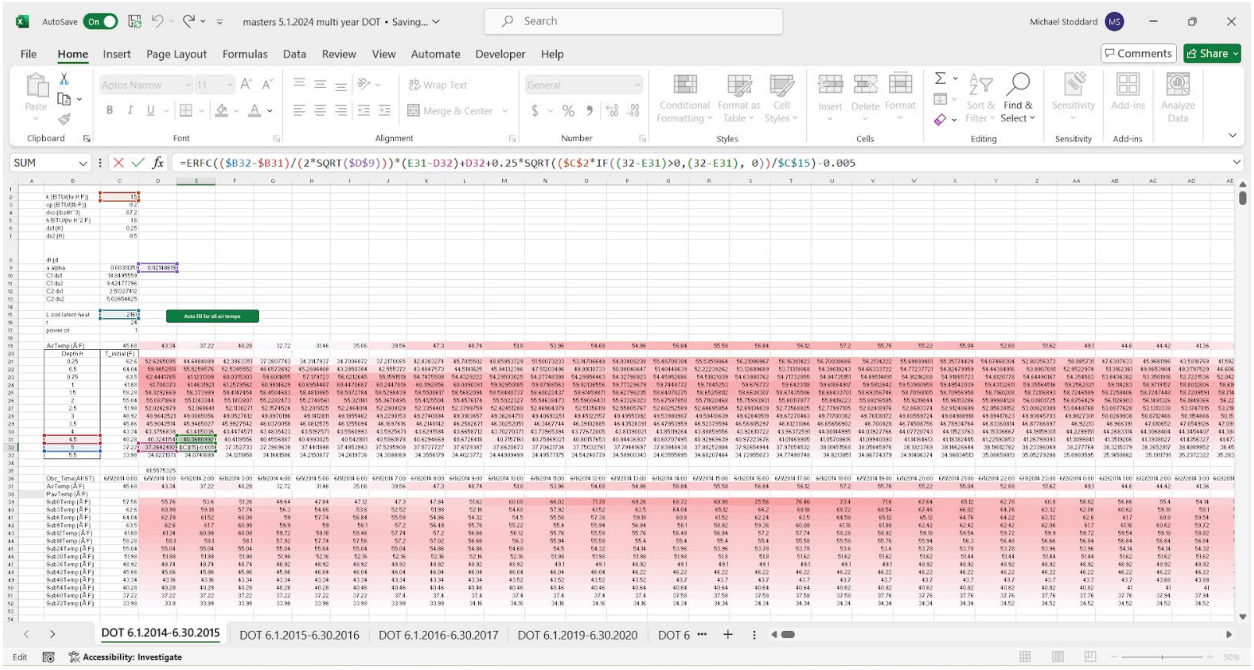

Figure 3 Illustration of a user interfacing with the model

Figure 4 below is a close-up section view of the temperature plotted as a function of time at the 1.0 depth (top) and 5-foot depth (bottom). The orange line is the simulated at-depth temperature, and the blue line is the actual temperature recorded from RWIS. The straight green line at 32 degrees Fahrenheit shows the bulk freezing temperature. The road material at 1-foot and 5-foot depth does not contain any appreciable unfrozen water below that temperature, and there is a negligible freezing point depression. Therefore, the green line is a fairly accurate location of the interface between unfrozen and frozen material. The red arrows nearer the right side of each plot show the predicted and actual time of thaw, which are nearly identical in this simulation.

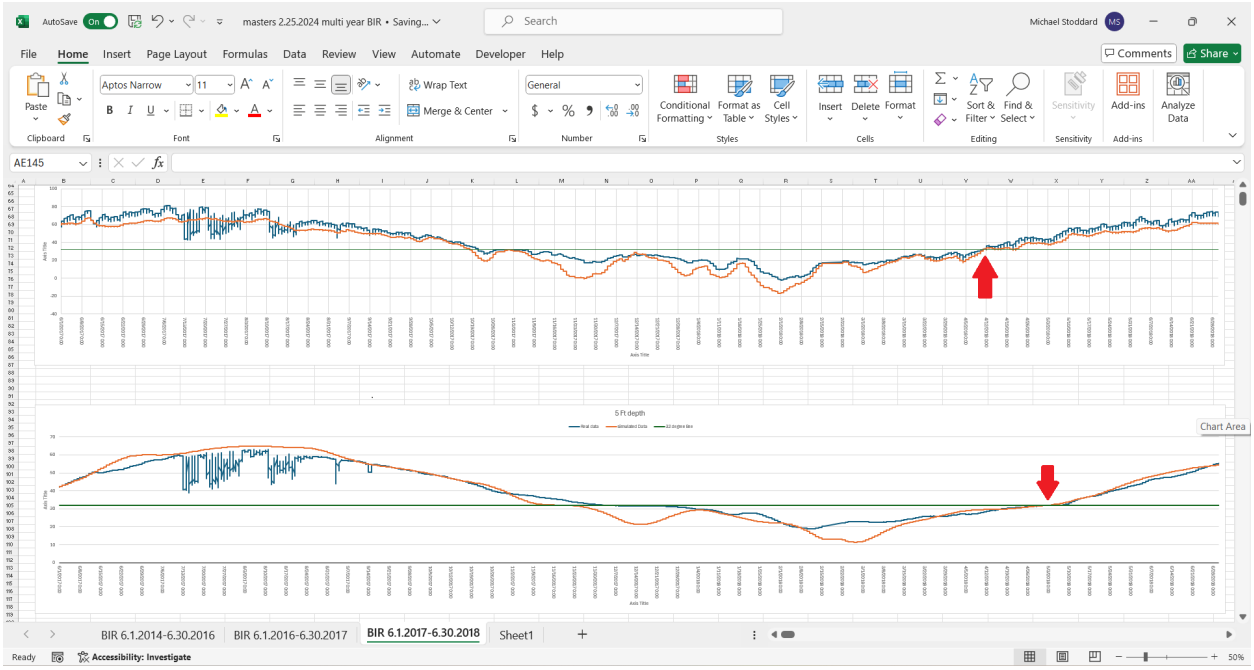

Figure 4 Scatter plots of the 1 foot and 5 foot depths, including the actual and model predictions

CHAPTER 4. FINDINGS

The model was calibrated and applied at four Alaska locations. In order to fully evaluate the predictive capability of the model, sufficient archived air, surface and subsurface temperature data are necessary Therefore, some sites (e.g. DOT Lake) had more comparison than others (e.g. Nenana Hills).

Each location was put into a separate copy of the master spreadsheet with tabs typically in one-year intervals due to the size constraint of Excel columns. The four sites used in this analysis are shows in the figure below:

- NEN- Parks Highway @ Nenana Hills MP 325.4
- DOT-Alaska Highway @ Dot Lake MP 1355.2
- CLR- Steese Highway @ Cleary Summit MP 20.9
- BIR- Richardson Highway @ Birch Lake MP 307.2

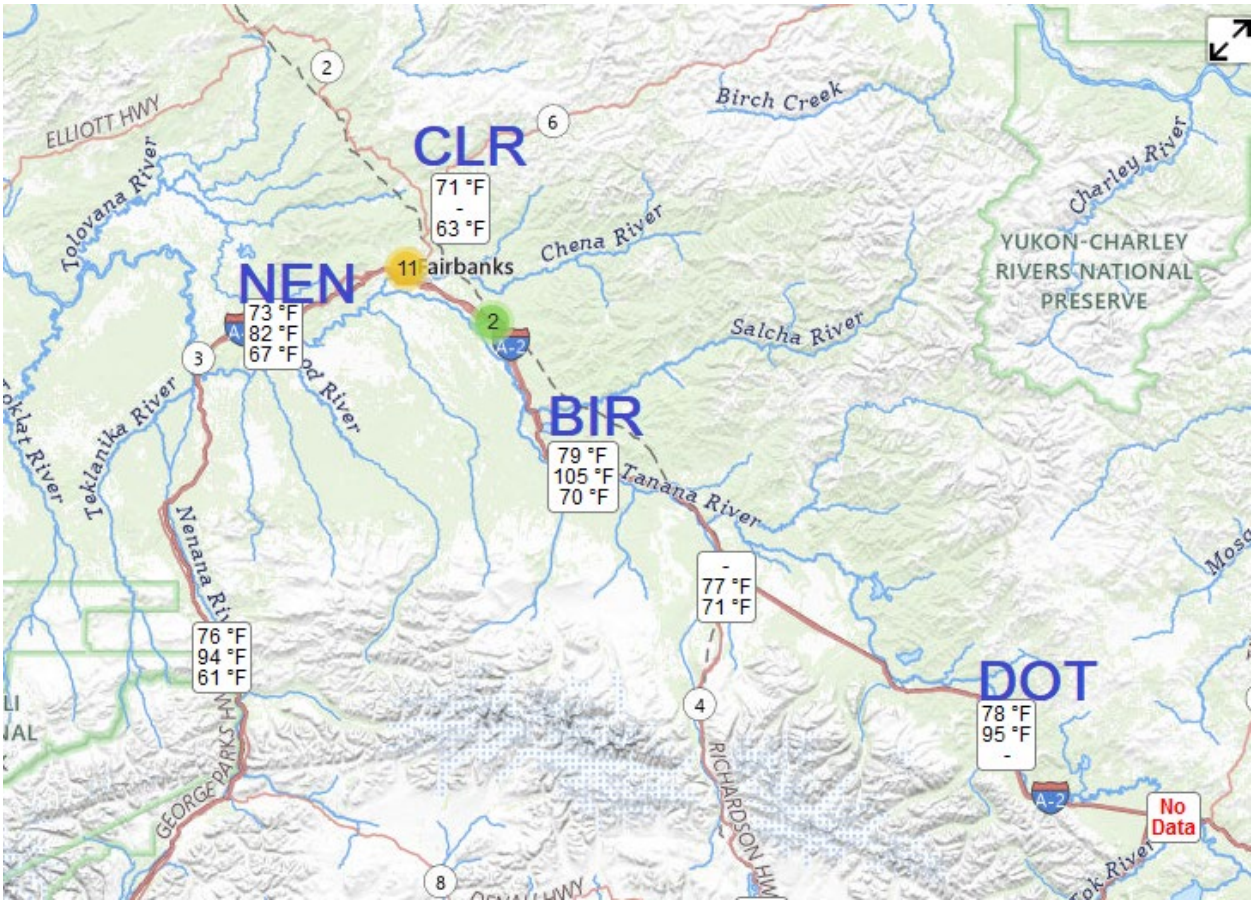

Figure 5 Map of the Interior of Alaska showing the four FWIS sites used in this analysis

Although the model predicts temperatures at all the depths discussed in section 4.1, the primary focus was on thaw at depths of 1.0 and 5.0 feet. Table 1 below summarizes the model performance for each of the sites analyzed.

Table 1 Summary of the predicted and actual dates of thaw for each site analyzed

Site	1 ft (model)	1ft (actual)	Error [d]	5 ft (model)	5 ft (actual)	Error [d]
NEN	4/12/18 17:00	4/12/18 22:00	0.21	5/6/18 5:00	5/12/18 20:00	6.63
DOT	4/8/15 19:00	4/14/15 18:00	5.96	5/6/15 11:00	5/16/15 3:00	9.67
	3/28/16 8:00	3/31/16 7:00	2.96	4/21/16 5:00	5/5/16 18:00	14.54
	4/15/20 21:00	4/20/20 19:00	4.92	5/6/20 1:00	5/14/20 6:00	8.21
	4/19/21 16:00	4/20/21 17:00	1.04	5/13/21 19:00	5/12/21 1:00	1.75
	4/25/22 10:00	4/25/22 8:00	0.08	5/17/22 4:00	5/21/22 5:00	4.04
BIR	3/27/15 13:00	4/3/15 22:00	7.375	N/A	N/A	N/A
	3/29/16 16:00	3/28/16 21:00	0.792	4/22/16 22:00	4/23/16 9:00	0.458
	4/5/17 20:00	4/5/17 20:00	0	4/30/17 18:00	5/3/17 9:00	2.63
	4/11/18 18:00	4/11/18 17:00	0.042	5/3/18 14:00	5/6/18 20:00	3.25
CLR	3/28/15 17:00	4/19/15 20:00	22.13	7/4/15 1:00	N/A	N/A
	4/6/16 15:00	4/11/16 21:00	5.25	4/22/16 15:00	5/13/16 14:00	20.96
	4/12/17 11:00	4/23/17 1:00	10.58	5/7/17 16:00	5/20/17 22:00	13.25
	4/26/18 10:00	4/23/18 22:00	2.5	5/14/18 21:00	5/25/18 20:00	10.96
	4/15/20 22:00	4/23/20 20:00	7.92	5/11/20 9:00	5/25/20 12:00	14.13

There is a row in the table for each year that there was sufficient data to do a comparison the model performance. Occasionally there were data gaps around the time of thaw that precluded a complete comparison; those are indicated with N/A in the table. The model time step used was one hour since that corresponds with the RWIS data resolution. Therefore, the date and time of thaw for both the model and the actual have an uncertainty of about 1 hour. As discussed in Section 4.3, the model can accommodate any time step and depends only on the resolution of the air temperature driving the simulation. The absolute difference between the model predictions and the actual thaw are shown in the Error column in units of days.

A summary of basic statistics of the error was calculated using all sites and all years, weighing each instance equally. A summary of these statistics is shown in Table 2 below.

Table 2 Statistic summary of the error

		1 foot error [d]	5 foot error [d]
Minimum		0	0.46
Maximum		22.13	20.96
Average		4.78	8.50

Predictions for the Cleary Summit (CLR) on the Steese highway had substantially more error than the other four sites; approximately double for all five years analyzed. Since CLR had one of the most comprehensive data sets (five years), the discrepancies of that site alone weigh more heavily in the statistics. Insets showing time of thaw at CLR are shown in Figure 5 below. It appears there is a larger

latent heat effect at this location and an adjustment of the thermal diffusivity would yield closer agreement, but the investigation is continuing as part of the larger graduate student's research project.

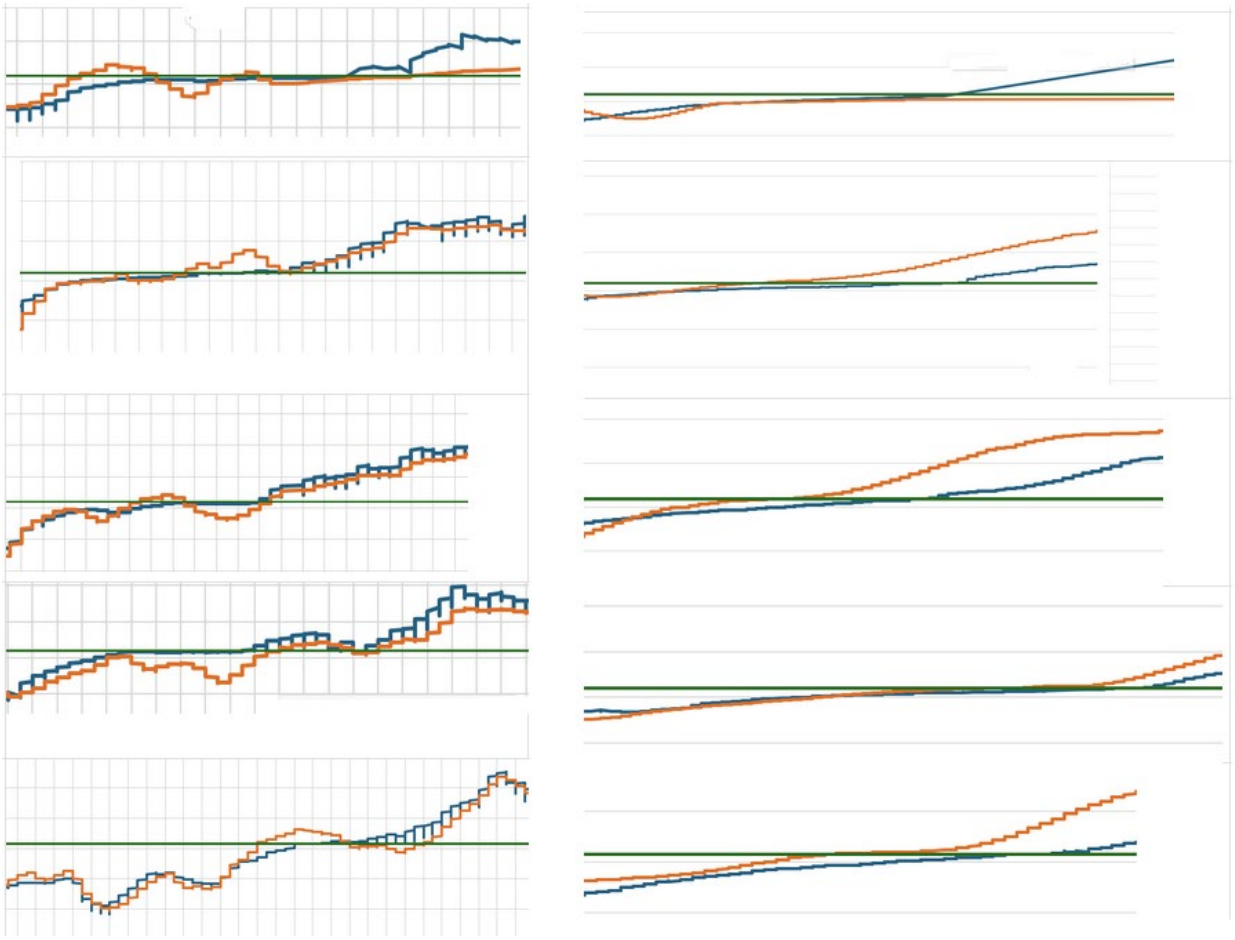

Figure 6 Model (yellow) and actual (blue) during thaw at 1 and 5 feet

CHAPTER 5. CONCLUSIONS

A numerical tool was developed that can fairly accurately predict the time of thaw at depth below a roadway using only surface air temperature data. The tool comes as an Excel spreadsheet and contains no macros or other external programs/scripts, so it can easily be used in many other major spreadsheet programs such as the free open-source LibreOffice Calc without modification. The uncertainty in the model is the same as the time resolution of the air temperature data driving the model. There is a single adjustable parameter that represents an effective thermal diffusivity that accounts for latent heat effects. A single value for this parameter was used in the analysis of CHAPTER 5, but an end user can easily adjust this value for a different site if there is some archived data available to validate it. We found a single value worked fairly well for the five sites analyzed because the subsurface material is likely similar at all sites. The average error at a depth of 1 foot was 4.78 days, and the average error at 5 feet was 8.5 days.

CHAPTER 6. REFERENCES

Comes-Pintaux, A. & Nguyen-Lamba, M., 1986. Finite-element enthalpy method for discrete phase change. *Numerical Heat Transfer,* 9(4), pp. 403-117.

Dall-Amico, M., Endrizi, S., Gruber, S. & Rigon, R., 2011. A robust and energy conserving model of freezing variably-saturated soil. *The Cryosphere,* Volume 5, pp. 469-484.

Goodrich, L. E., 1978. Efficient numerical technique for one-dimensional thermal problems with phase change. *International Journal of Heat and Mass Transfer,* 21(5), pp. 615-621.

Hansson, K., Simunek, J. M. M. & Lundin, L.-C., 2004. Water flow and heat transport in frozen soil: Numerical solution and freeze-thaw applications. *Vadose Zone,* Volume 3, pp. 693-704.

Harlan, R., 1973. Analysis of coupled heat-fluid transport in partially frozen soil. *Water Resources Research,* 9(5), pp. 1314-1323.

Jame, Y. & Norum, D., 1980. Heat ans mass transfer in a freezing unstaturated porous medium. *Water Resources Research,* 16(4), pp. 811-819.

Jumikis, A. R., 1977. *Thermal Geotechnics.* New Brunswick: Rutgers Univ. Press.

Konrad, J. & Morgenstern, N., 1984. Frost heave prediction of chilled pipelines buried in unfrozen soils. *Canadian Geotechnical Journal,* 21(1), pp. 100-115.

Kozlowski, T., 2001. A finite difference scheme to solve one-dimensional problems associated with soil freezing and thawing. *Archives of Hydroengineering and Geomechanics,* 46(4), pp. 113-131.

Nixon, J., 1975. The role of convective heat transport in the thawing of soils. *Canadian Geotechnical Journal,* 12(3), pp. 425-429.

Riseborough, D. & Smith, M., 1985. *The sensitivity of thermal predictions to assumptions in soil properties.* Rotterdam/Boston, s.n.

Transportation Research Board, 2010. *NCHRP Report 672 - Roundabouts: An Informational Guide - 2nd Edition,* Washington, D.C.: Transportation Research Board of the National Academies.